

# Thermic transformation of sillimanite single crystals to 3:2 mullite plus melt: investigations by polarized IR-reflection micro spectroscopy

C.H. Rüscher

*Institut für Mineralogie, Universität Hannover, Welfengarten 1, 30167 Hannover, Germany*

## Abstract

Oriented and polished high quality sillimanite single crystals were thermally treated for 4, 24 and 96 h at 1600°C. The products were quenched to room temperature and investigated using polarized IR microspectroscopy in reflection mode (600–4000 cm<sup>-1</sup>). The spectra of the 24 and 96 h thermally treated sample indicates the transformation of sillimanite to 3:2 mullite plus melt of eutectic SiO<sub>2</sub>/Al<sub>2</sub>O<sub>3</sub> composition. The anisotropy of the spectra show a high degree of orientation of crystals according to a topotaxial reaction. The high wavenumber mullite lattice bands between 1100 and 1200 cm<sup>-1</sup> are assigned to modes of [SiO<sub>4</sub>] units interconnected within the mullite specific (Al\*SiAl–O<sub>c</sub>\*) 3-clusters, and Si–O<sub>c</sub>–Si- and Si–O<sub>c</sub>–Al-bonds. It is shown that the sillimanite to mullite transformation occurs by an increased damping of all modes of the sillimanite lattice due to an irreversible increase of anharmonicity preserved as a typical property of mullite. © 2001 Elsevier Science Ltd. All rights reserved.

*Keywords:* Mullite; Sillimanite; Spectroscopy

## 1. Introduction

Mullite and sillimanite are structurally closely related.<sup>1,2</sup> The structural relation is obvious not only from the (AlO<sub>6</sub>) octahedra which form in both structures chains of top chaired building units infinitely extended along the *c* direction. Additionally, the tetrahedral units which form double chains with a perfect order of Al and Si in the sillimanite structure are also found in mullite, however, with the absence of perfect order and interrupted by oxygen vacancies and the formation of 3-clusters of tetrahedral units. It has been shown in earlier single crystal X-ray investigations that sillimanite transforms into 3:2 mullite at temperatures of about 1600°C.<sup>3</sup> This transformation is just what can be expected according to the Al<sub>2</sub>O<sub>3</sub>–SiO<sub>2</sub> phase diagram. Heating a starting composition of 1:1 Al<sub>2</sub>O<sub>3</sub>/SiO<sub>2</sub> as given by sillimanite at 1600°C thus invariably lead to melt of eutectic composition coexisting with 3:2 mullite. Therefore, partial melting could be assumed to be important for the final appearance of mullite. Another interesting question concerns the initial steps for this transformation. It is clear that in a step before melt formation Si<sup>4+</sup> and O<sup>2-</sup> should become enriched and Al<sup>3+</sup> exhausted in certain areas. On the other hand the formation of mullite requires the removal of O<sup>2-</sup> and Si<sup>4+</sup> and the supply of Al<sup>3+</sup> for charge neutrality. Guse et al.<sup>3</sup> suggest a high

stability of the octahedral chains unaffected during the thermal transformation. Therefore, these authors assume a topotaxial reaction with a high degree of orientation of mullite crystals according to the close similarity of both structures. Further on, these authors propose a transformation scheme according to the decomposition of sillimanite into a so called “transition mullite”, which could be Al richer than the final 3:2 mullite. The “transition mullite” and sillimanite coexist before sillimanite breaks down completely and 3:2 mullite appears. This indicates that the transformation occurs rather inhomogeneously within the crystal governed by inhomogeneities of the crystal rather than being an intrinsic reaction.

The thermic transformation of sillimanite to mullite has been reinvestigated at our department in several approaches using predominantly TEM techniques<sup>4–6</sup> and IR methods.<sup>7,8</sup> Some new results obtained by TEM experiments together with structure simulations indicating the effect of Si/Al disordering prior to mullitization are reported by Rahman et al.<sup>9</sup> (this issue). The results obtained by IR-reflection spectroscopy are outlined here. The new point presented is that polarized IR reflection micro spectroscopy can be used easily to obtain informations about the thermal transformation of sillimanite and mullite, including the respective orientations of the 3:2 mullite crystals and the sillimanite starting material.

A success is also that first “single crystal” reflectivity data of 3:2 mullite are obtained. An assignment of the high frequency lattice modes (compare Refs. 10–13) and the initial state of mullitization of sillimanite is discussed.

## 2. Experimental

A high quality, clear and colourless sillimanite single crystal (Sri Lanka) was oriented cut into pieces of sizes  $1 \times 0.5 \times 0.1$  mm. The larger 010 surfaces of each piece were polished and checked for their orientation by polarized IR reflection spectroscopy using a specifically designed microscope attached to an FTIR spectrometer (Brüker IFS 88, IR-scope I A 590, KRS5 polarizer, Al mirror for 100% reference). The lower spectral range for these measurements was restricted to  $600 \text{ cm}^{-1}$  by using the microscope technique. The upper limit was  $4000 \text{ cm}^{-1}$ . Since above  $1300 \text{ cm}^{-1}$  no absorption effect was seen and the interference pattern (multiple reflection) observed for the clear samples are not used for the further analysis, the spectra are shown only up to  $1300 \text{ cm}^{-1}$ . Using the microscope technique had the advantage that selected areas of the crystal could be investigated. Spot sizes of  $90 \mu\text{m}$  in diameter were used for the measurements. Three crystal pieces were treated at  $1600^\circ\text{C}$  for 4 h and two other crystal pieces for 24 and 96 h, respectively. The samples were quenched to room temperature by taking them out of the furnace. Polarized reflectivities of a mullite 2:1 crystal were measured for comparison.

## 3. Results

Polarized reflection spectra of the thermally treated sillimanite (24 h and 96 h) are shown in Fig. 1. Plotted are the spectra  $R_a$  (top) and  $R_c$  (bottom) of the main directions, which are given by

$$R(\theta) = R_a \cos^2 \theta + R_c \sin^2 \theta \quad (1)$$

indicating the typical effect of an anisotropic crystal.  $\theta$  is measured as the relative angle of the polarisation of the incident electric field ( $E$ ) with respect to the direction  $a$  or  $c$  of the crystal. The orientations of  $R_a$  and  $R_c$  correspond well to  $R_a//a$  and  $R_c//c$  of the sillimanite starting material (unit cell setting Pbnm) within experimental error ( $\pm 2^\circ$ ). Comparison to appropriate spectra of 2:1 mullite single crystals (Fig. 1) shows a good agreement in characteristic reflection bands but also significant differences in some details. The good agreement indicates that mullite has formed and that the crystallographic orientation of the newly formed mullite well corresponds to the related directions in sillimanite.

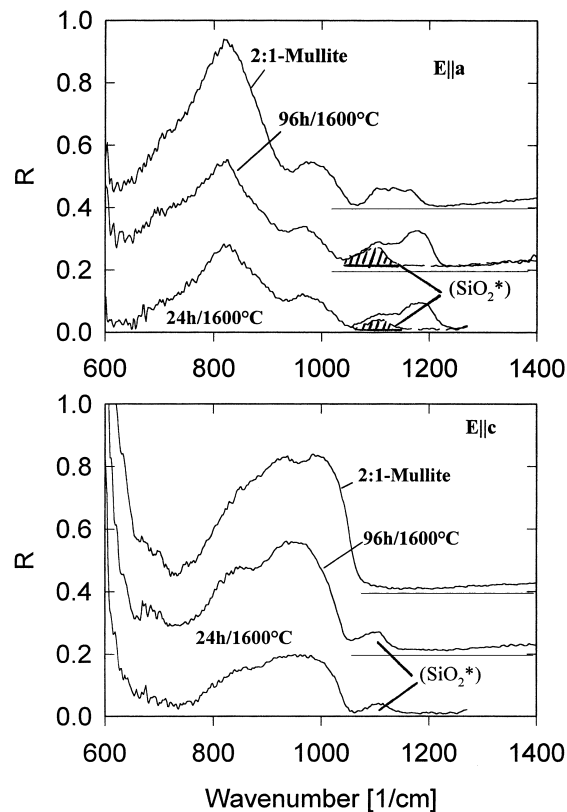


Fig. 1. Polarized reflectivity of thermally treated sillimanite at  $1600^\circ\text{C}$  for 24 and 96 h and of a 2:1 mullite single crystal. Spectra are shifted vertically:  $\text{SiO}_2^*$  glass is obtained as isotropic contribution marked by dashed area in the top figure (\*denotes Al incorporated, see text).

It may be noted that the thermally treated sample looks completely milky white, which can be explained by diffuse reflection due to the presence of surfaces of many intergrown crystals. Deviations of the orientations of mullite crystals from the sillimanite “parent” crystal are, however, less than  $\pm 2^\circ$  for more than about 99% of the sample.

The detailed differences observed in the reflection bands between  $1050$  and  $1250 \text{ cm}^{-1}$  can be explained by the formation of 3:2 mullite together with the presence of glass with eutectic composition. The glass contribution was determined in all cases for the  $a$ – $c$  plane rotating the sample slice in steps of  $10^\circ$  with respect to the polarisation field. In doing so the isotropic contribution can be seen as that part which does not follow Eq. (1). The peak maximum of the isotropic contribution is at about  $1105 \text{ cm}^{-1}$  whereas the reflection of pure  $\text{SiO}_2$ -glass is peaked at  $1123 \text{ cm}^{-1}$ . The lower peak position is a signature of the incorporation of Al.<sup>14</sup> For pure  $\text{SiO}_2$  the reflectivity at peak maximum is measured to be as large as ca. 70%. By assuming an ideal exsolution of sillimanite into 3:2 mullite plus melt of eutectic composition a volume fraction of glass of about 17% can be expected. Therefore, a maximal contribution of

$R \approx 12\%$  can be expected for the reflectivity of the glass part of the thermally treated sillimanite. It may be noted that the reflectivity of the thermally treated samples was measured without further polishing of the surface. A maximal scattering loss might be estimated to about 40% comparing the observed spectra for 2:1 mullite and the 96 h heat treated sillimanite in the range between 700 and 1050  $\text{cm}^{-1}$ . Thus, it can be concluded that the observed peak height of  $R = 5\text{--}8\%$  is very close to the expected ideal value. However, a more precise quantification of the absolute glass contribution is difficult by using such kind of measurements without a further investigations of the effect of glass contribution in reflection spectra.

Crystals thermally treated for 4 h at 1600°C appear in the optical microscope inhomogeneously composed of milky white and clear areas. Selected reflection spectra (A, B, C) obtained on clear areas are shown for their main direction [eq. (1)] in Fig. 2 in comparison to spectra of the sillimanite starting material. The spectra indicate a gradual decrease of all sillimanite characteristic bands. In particular the bands peaked at 900, 990 and 1190  $\text{cm}^{-1}$  for  $E//a$  and at 700  $\text{cm}^{-1}$  for  $E//c$  reduces to 20% of their initial reflection value. The band around 900  $\text{cm}^{-1}$  reduces to about 40% and simultaneously a

shoulder appears in the low frequency side at about 800  $\text{cm}^{-1}$ . The decrease of the band around 800  $\text{cm}^{-1}$  in the  $E//a$  spectra tends to saturate at about 55% of the initial value. The additional features observed for samples A, B and C between 1050 and 1150  $\text{cm}^{-1}$  in the  $E//a$  spectra are absent for  $E//c$  like the characteristic peak of stronger intensity at around 1190  $\text{cm}^{-1}$  for sillimanite. Although small in intensity, these features are rather significant for samples A, B and C and it has been checked that these features follow the anisotropic behaviour according to Eq. (1). Even an additional isotropic contribution of lower intensity could be observed in the spectra of sample C between 1050 and 1110  $\text{cm}^{-1}$ . These details will be further discussed below together with a quantification of the spectral changes.

## 4. Discussion

### 4.1. Single crystal reflection spectra of mullite

The spectra obtained for thermally treated sillimanite for 24 and 96 h show that mullite of composition 3:2 and melt of eutectic composition has formed in support of the implication of the  $\text{Al}_2\text{O}_3\text{--SiO}_2$  phase diagram. The orientation of the mullite crystals well agrees with the appropriate sillimanite axis thus indicating a topotaxial reaction. This observation is in agreement with results reported by Guse et al.<sup>3</sup> using single crystal X-ray investigation which were confirmed in further investigations using X-ray diffraction techniques and transmission-electron microscopy.<sup>4–6</sup> Although not single crystal, the reflection spectra obtained for the thermally treated sillimanite for 24 and 96 h (Fig. 1) do show quasi single crystal features. This is of some interest because single crystals data exist only for 2:1 mullite<sup>13</sup> but could not be measured for 3:2 mullite because of too small crystal sizes available. A higher Si/Al ratio for 3:2 compared to 2:1 mullite is shown by the intensity distribution between 1050 and 1250  $\text{cm}^{-1}$  in the  $E//a$  spectra. For sillimanite the appropriate transversal optical mode with its peak maximum at  $\omega = 1170 \text{ cm}^{-1}$  in the imaginary dielectric function ( $\epsilon''$ ) has been assigned to an internal vibration of the  $\text{SiO}_4$  tetrahedra.<sup>15</sup> The particular high wavenumber could be an indication of the very short Si– $\text{O}_c$  distance of about 157 pm.  $\text{O}_c$  denotes the  $\text{SiO}_4$  and  $\text{AlO}_4$  interconnecting oxygen. The related Al– $\text{O}_c$  distance reads 171 pm. Average bond lengths are about 161 pm and 175 pm for the ( $\text{SiO}_4$ ) and ( $\text{AlO}_4$ ) tetrahedral units, respectively (these structural details are known, e.g. Ref. 2). The close similarity in peak position of the high wavenumber reflection band for sillimanite and 3:2 mullite (compare Fig. 1 and Fig. 2) implies an analogue assignment for both bands. Following this line of arguments leads to the conclusion that there are rather similar ( $\text{SiO}_4$ ) tetrahedral environments

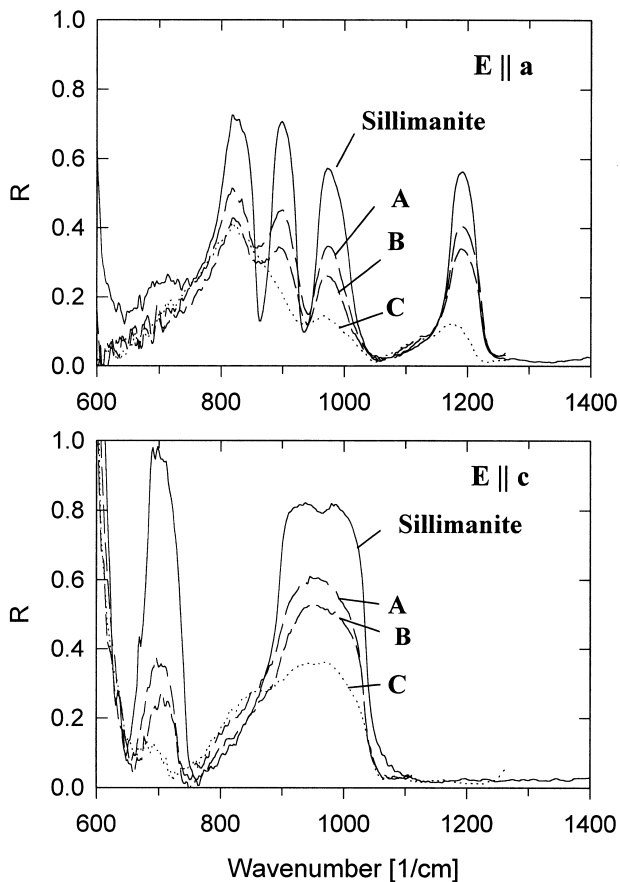


Fig. 2. Polarized single crystal reflectivity of sillimanite and of thermally treated sillimanite crystals A, B, C for 4 h at 1600°C (compare text).

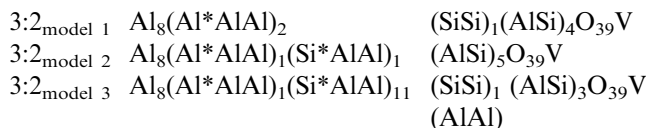
in sillimanite and 3:2 mullite with respect to the interconnection Si–O<sub>c</sub>–Al. It is clear that mullitization is essentially related to the formation of T\*TT 3-clusters around an O<sub>c</sub>\* oxygen and to the formation of oxygen vacancies. Accordingly, the number of Si–O<sub>c</sub>–Al units (i.e. the appropriate amount of short Si–O<sub>c</sub> distances) is lower in 3:2 mullite compared to sillimanite which explains the reduced intensity of the high wavenumber reflection band. A high wavenumber reflection band with a very similar wavenumber of the appropriate transversal optical mode as deduced from the spectra of sillimanite and 3:2 mullite (see below, Table 1) is also obtained for 2:1 mullite ( $\omega = 1162 \text{ cm}^{-1}$  compare Ref. 13). Thus there are “sillimanite” type Si–O<sub>c</sub>–Al units present also in 2:1 mullite. The assumption of short effective Si–O bond length present in mullite is supported by single crystal structure determinations of 2:1 mullite carried out using X-ray<sup>2</sup> as well as neutron diffraction techniques.<sup>16</sup> In Refs. 2 and 16 it is shown that sillimanite like short Si–O distances are very evident for the real structure of mullite, which are observed introducing split atomic positions. This effect can, however, not be seen in structure determination on the basis of the mullite average structure.

In the  $E//a$  reflection spectra of 3:2 mullite there is an additional intensity contribution between 1100 and 1150  $\text{cm}^{-1}$ , which becomes obvious subtracting the glass peak (marked in Fig. 1). The assumption of more than one absorption band situated in 3:2 mullite between 1100 and 1200  $\text{cm}^{-1}$  is supported from IR powder spectra.<sup>10–12</sup> It is also known from single crystal reflection spectra of 2:1 mullite<sup>13</sup> that there are three lattice bands which are peaked at 1108, 1133 and 1162  $\text{cm}^{-1}$  in the  $E//a$  and  $E//b$  polarized spectra. The related triplicate structure in the reflection spectra of 2:1 mullite can well be observed by direct inspection of Fig. 1. An assignment of these bands has been discussed as to be due to (Al\*O<sub>4</sub>), (AlO<sub>4</sub>) and (SiO<sub>4</sub>) structural units and to their complex interconnections. It has been observed in IR investigations on Al mullites (no Si on T positions) that the reflection bands above 1100  $\text{cm}^{-1}$  are completely absent.<sup>17</sup> Therefore, any assignment of these bands should have a particular emphasize to the SiO<sub>4</sub> tetrahedral units.

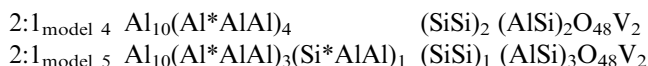
The presence of Si–O<sub>c</sub>–Si building units has been found by computer simulations as a most stable atomic ordering scheme above and below an oxygen vacancy in a sillimanite lattice.<sup>18</sup> Such a configuration should lead to a somewhat lower wavenumber position of the appropriate (SiO<sub>4</sub>) internal mode compared to the (SiO<sub>4</sub>) tetrahedra in the sillimanite type Si–O<sub>c</sub>–Al configuration according to relaxed Si–O distances. Different Si–O distances can also be expected for (Si\*O<sub>4</sub>) units, denoted as Si\*AlAl 3-cluster or for an (SiO<sub>4</sub>) within an Al\*AlSi-3-cluster configuration (i.e. three tetrahedra interconnected by O<sub>c</sub>\*). An overview of the possible

configurations is obtained rewriting the mullite formula for the average structure  $\text{Al}_2\text{Al}_{2+2x}\text{Si}_{2-2x}\text{O}_{10-x}\text{V}_x$  ( $x$  = number of oxygen vacancies V) as follows:

for 3:2 mullite,  $x = 0.25$ , rewritten for 4 unit cells:



for 2:1 mullite,  $x = 0.4$ , rewritten for 5 unit cells:



The configurations given by model 1–5 may be extended by further assumptions taking into account configurations like (Al\*AlSi), (Al\*SiSi) or (Si\*SiSi). The composition  $x$  may also be varied. Single crystal structure refinement from X-ray data<sup>2</sup> and neutron diffraction<sup>16</sup> have shown that up to 30% of Al\* atoms could be replaced by Si atoms for 2:1 mullite. Taking into account the results of mullite single crystal determinations and configurations shown by Padlewski et al.<sup>18</sup> as most stable around an oxygen vacancy in sillimanite, (Si,Si) and (Al\*AlAl), the models 1–5 may be used as a first approximation in order to explain the intensity distribution in the high frequency reflection band of 2:1 and 3:2 mullite. According to model 1 Si–O<sub>c</sub>–Si and Al–O<sub>c</sub>–Si are distributed in mullite of relative portions of 1:4. The high frequency dominating peak should be assigned to the portion of Si–O<sub>c</sub>–Al, as can be suggested from the close similarity to the sillimanite spectra. It can not be ruled out that 3:2 mullite also possess three peaks. However, the third peak at lower wavenumber certainly shows rather low intensity. This conclusion is supported by the appearance of IR-powder spectra of 3:2 mullite.<sup>12</sup> A third peak could also be taken into account by mixing the model configurations 1 and 2. Configurations as given by model 3 may be unfavourable because of Al–O<sub>c</sub>–Al interconnections. For 2:1 mullite model 5 could explain the intensity distribution most favourable according to the appearance of three peaks in the range 1100–1200  $\text{cm}^{-1}$ . It may be noted that rearrangements of configurations, e.g. between model 4 and 5 or between 1, 2 or 3 should change the intensity distribution in the high wavenumber peaks without changing the chemistry, which could be a complication for the determination of Si/Al ratios by IR spectra.<sup>12</sup>

#### 4.2. The initial step of mullitization of sillimanite in IR spectra

The initial step of mullitization of sillimanite at 1600°C is indicated in the IR spectra by the breakdown

of all reflection bands (Fig. 2). The main question is whether this breakdown is due to a loss of oscillator strength or if it is related to the damping of the oscillators. Some preliminary calculations were carried out using Kramers Kronig analysis (compare Ref. 13 for using the Kramers Kronig analysis for data evaluation of 2:1 mullite). The calculated imaginary part of the dielectric function indicate a gradual broadening and decrease of peak height of the appropriate transversal modes peaked at about  $\omega = 809, 883, 960$  and  $1160\text{--}1170\text{ cm}^{-1}$ . A new broad absorption band appears between  $1050\text{--}1150\text{ cm}^{-1}$ , which is also directly observed in the reflection spectra. Because of the limited range of the spectra and the uncertainties in the extrapolation procedures the result obtained by Kramers Kronig analysis could, however, not be used for a further evaluation of the spectra. Therefore, direct calculation of the reflectivity were carried out using the complete data set known for sillimanite lattice bands.<sup>13</sup> The curves obtained manipulating appropriate values of the sillimanite data set by trial and error are plotted in Fig. 3 in comparison to the curves for sillimanite. A very good agreement with the experimental findings for curves A, B, C and for sillimanite (Fig. 2) is obtained. According to this the initial step of thermal transformation at  $1600^\circ\text{C}$  of sillimanite is related with the irreversible broadening of all lattice bands as given in Table 1 for the damping constants  $\gamma_i$ . It can be seen that a systematic increase of  $\gamma_i$  is sufficient to describe the spectra A and B. It can also be seen that oscillator strength is lost significantly only for the mode  $\omega_i = 684\text{ cm}^{-1}$  for  $E//c$ . However two additional oscillators, one for  $E//a$  at about  $1130\text{ cm}^{-1}$  and one for  $E//c$  at about  $840\text{ cm}^{-1}$  were introduced in order to describe tentatively the new features which come up on thermic treatment. It may be noted that the marked positions agree with lattice oscillator frequencies of mullite. However, it may be ruled out that any mullite has formed at this stage of reaction for those areas of the

Table 1

Values used for calculations of reflectivity spectra 1–4 in Fig. 3:  $\omega_i$  = oscillator frequency (in  $\text{cm}^{-1}$ ),  $\gamma_i$  = damping constant (in  $\text{cm}^{-1}$ ),  $F_i$  = oscillator strength. (Values for spectra 1 as given in Ref. 13 for sillimanite)

| 1           |            |       | 2          |            |       | 3          |            |       | 4          |            |       |
|-------------|------------|-------|------------|------------|-------|------------|------------|-------|------------|------------|-------|
| $\omega_i$  | $\gamma_i$ | $F_i$ | $\omega_i$ | $\gamma_i$ | $F_i$ | $\omega_i$ | $\gamma_i$ | $F_i$ | $\omega_i$ | $\gamma_i$ | $F_i$ |
| <i>E//a</i> |            |       |            |            |       |            |            |       |            |            |       |
| 1174        | 10         | 0.1   | 1174       | 20         | 0.1   | 1174       | 25         | 0.1   | 1174       | 50         | 0.075 |
|             |            |       | 1130       | 40         | 0.01  | 1130       | 40         | 0.01  | 1130       | 40         | 0.015 |
| 960         | 15         | 0.08  | 960        | 30         | 0.08  | 960        | 50         | 0.08  | 960        | 80         | 0.08  |
| 883         | 8          | 0.2   | 883        | 30         | 0.2   | 883        | 50         | 0.2   | 883        | 80         | 0.08  |
| 809         | 19         | 0.6   | 809        | 30         | 0.6   | 809        | 50         | 0.6   | 800        | 60         | 0.6   |
| <i>E//c</i> |            |       |            |            |       |            |            |       |            |            |       |
| 900         | 14         | 0.66  | 900        | 40         | 0.66  | 915        | 50         | 0.6   | 925        | 80         | 0.55  |
|             |            |       | 840        | 40         | 0.05  | 840        | 40         | 0.05  | 840        | 60         | 0.13  |
| 684         | 9          | 0.6   | 684        | 30         | 0.3   | 684        | 40         | 0.25  | 684        | 60         | 0.1   |

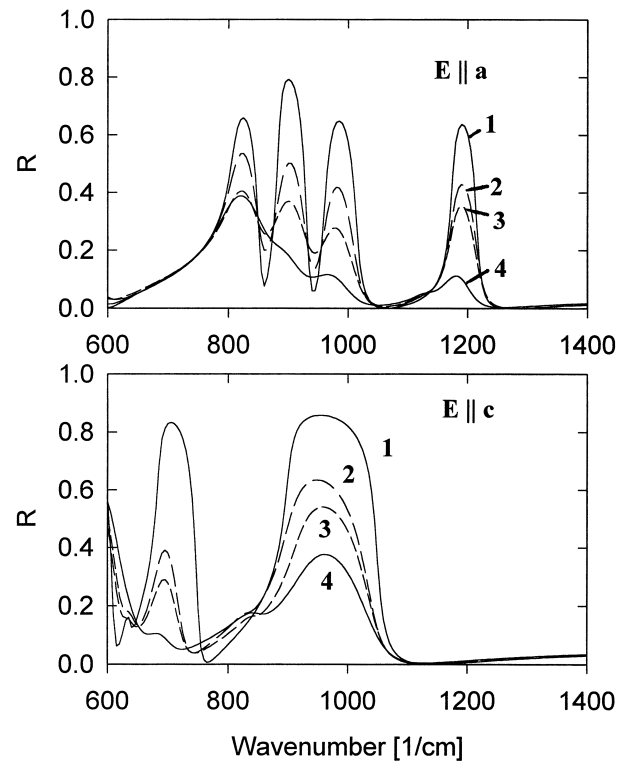


Fig. 3. Four curves of calculated reflectivity. Parameter values for curves 1–4 are listed in Table 1.

crystal investigated by IR-microscope technique. The absence of mullite in the initial state is also concluded from results of TEM investigation, both in diffraction as well as in high resolution imaging.<sup>9</sup>

An initial weakening of all diffraction peaks with  $l=2n+1$  and the absence of these diffraction peaks before mullite forms has been reported.<sup>3–6,9</sup> This has been explained by Rahman et al.<sup>9</sup> by introducing split atomic positions for  $\text{O}_c$ , which could be correlated with a partial disorder of Al and Si on T sites. Such an effect clearly might be described by a long range order parameter  $Q_{\text{LO}} = 1$  for a perfectly ordered state and by  $< Q_{\text{LO}} < 1$  for sillimanite after some time held at  $1600^\circ\text{C}$ . The number of symmetry allowed modes now reduces to that of the ideal sillimanite structure containing disordered Si/Al distribution as  $Q$  tends to zero. Therefore, all IR-modes forbidden by symmetry for the ideal sillimanite (half the sillimanite unit cell) will disappear rapidly with advanced reaction state. The rapid decrease in intensity of the mode at  $\omega = 684\text{ cm}^{-1}$  can be taken as a support for this interpretation. Another support is given by inspecting reflection spectra of all main components for mullite and sillimanite. In Fig. 4 of Ref. 13 it can be seen that the number of leading reflection modes has been reduced in 2:1 mullite compared to sillimanite. It is interesting to note that the loss of oscillator strength occurs initially in a mode for  $E//c$  ( $\omega = 684\text{ cm}^{-1}$ ) and later in the reaction path in  $E//a$  ( $\omega = 883\text{ cm}^{-1}$ ,

Table 1). This indicates that the IR pattern reacts more sensitive for the loss of Al/Si order in  $c$  direction

The second point to be explained is the peak broadening, which comes up irreversibly for thermally treated sillimanite. Such a peak broadening can be interpreted as an ingredient of increasing anharmonicity of the lattice, which can be due to the creation of point defects together with quasi stable interstitials. Therefore, it is claimed that the appearance of additional features in the spectra, around  $840$  and  $1130\text{ cm}^{-1}$  are due to  $T^*$  occupation and the formation of  $T$  vacancies. The hopping of an Al to  $Al^*$  leaves behind an  $Si-O_c-V_{Al}$  ( $V_{Al}$  = Al-vacancy) with relaxed Si–O distances, which could be a good candidate for absorption at about  $1130\text{ cm}^{-1}$ . It cannot, however, be ruled out presently that local configurations  $Si-O_c-Si$  could also be formed, which could gain absorption intensity around  $1130\text{ cm}^{-1}$ . Nevertheless, the peak broadening of the lattice modes is irreversible and is preserved for the mullite state as an particular state of matter, i.e. the anharmonicity in the bonding is preserved.

The transformation to mullite can be seen in the next step comparing the spectra of sample C to that of thermally treated sillimanite for 24 h (Fig. 4). The main point here is that the mullite lattice has to be created or

with other words the contributions of  $T^*$  point defects should become lattice vibrations. This can only occur via the formation of oxygen vacancies and the enrichment of Al and exhaustion of Si by the formation of structure gradients. In spectra C a small isotropic contribution peaked at about  $1080\text{ cm}^{-1}$  can be seen. This indicates the presence of an amorphous contribution richer in Al compared to the eutectic composition as a possible precursor form to the formation of melt. For the 24 h thermally treated sample the peak indicating melt formation is significant larger in intensity and the contribution assigned to  $Si-O_c-V_{Al}$  units in the sillimanite matrix should decrease forming glass like networks. It is concluded that the intrinsic thermic transformation of sillimanite to mullite is controlled by solid state diffusion and that melt forms in a secondary step. The formation of first melt, however, should accelerate the transformation.

### Acknowledgements

The DFG is thanked for support (Schwerpunktprogramm Strukturgradienten, Ru 764/3-1). Professor Schneider (DLR Köln) is thanked for support concerning the mullite crystals and several helpful discussions.

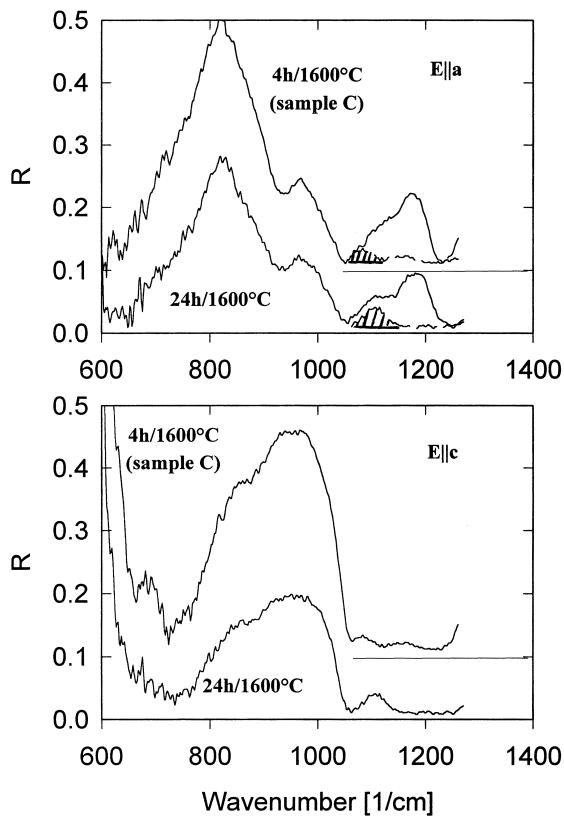


Fig. 4. Comparison of reflectivity spectra C (adapted from Fig. 2) and for the sample 24 h/1600°C (adapted from Fig. 1). (Isotropic contribution marked in top figure by dashed area.)

### References

- Sadanaga, R., Tokonami, M. and Takeuchi, Y., The structure of mullite,  $2Al_2O_3 \cdot SiO_2$ , and relationship with the structures of Sillimanite and Andalusite. *Acta Crystallogr.*, 1962, **15**, 65–68.
- Angel, R. J. and Prewitt, C. T., Crystal structure of mullite: a reexamination of the average structure. *Am. Mineral.*, 1986, **71**, 1476–1482.
- Guse, W., Saalfeld, H. and Tjandra, J., Thermal transformation of sillimanite single crystals. *N. Jb. Miner. Mh.*, 1979, **4**, 175–181.
- Fröhlich, A., Elektronenmikroskopische und röntgenographische Untersuchungen zum Phasenübergang Sillimanit nach Mullit. PhD thesis, Universität Hannover, Germany, 1990, 1–78.
- Koithan, H., *Initialstadium der thermischen Umwandlung von Sillimanit in Mullit*. PhD thesis, Universität Hannover, Germany, 1994, 1–106.
- Feustel, U., Strukturelle Beschreibung der thermischen Umwandlung von Sillimanit in Mullit. PhD thesis, Universität Hannover, Germany, 1996, 1–88.
- Feustel, U., Rahman, S. H. and Rüscher, C. H., IR investigations of the sillimanite to mullite transformation. *Eur. J. Mineral.*, 1996, **8**, 54.
- Rüscher, C. H., Nachweise kohärenter und nicht-kohärenter Eigenschaften mit Hilfe der optischen Spektroskopie an Mullit, Sulfiden des Typs  $(MS)_nTS_2$  und Fe-reichen, natürlichen Biotiten. Habilitationsschrift, Universität Hannover, Germany, 1997, Kap. 3, 13–32.
- Rahman, S., Feustel, U. and Freimann, S., Structure description of the thermic phase transformation sillimanite–mullite. *J. Eur. Ceram. Soc.*, 2001, **21**(14), 2471–2478.
- MacKenzie, K. J. D., Infrared frequency calculations for ideal mullite ( $3Al_2O_3 \cdot 2SiO_2$ ). *J. Am. Ceram. Soc.*, 1979, **55**, 68–70.
- Cameron, W. E., Composition and cell dimensions of mullite. *Am. Ceram. Soc. Bull.*, 1977, **56**, 1003–1011.

12. Rüscher, C. H., Schrader, G. and Götte, M., Infra-red spectroscopic investigations in the mullite field of composition:  $\text{Al}_2(\text{Al}_{2-2x}\text{Si}_{2-2x})\text{O}_{10-x}$  with  $0.55 > x > 0.25$ . *J. Eur. Ceram. Soc.*, 1996, **16**, 169–175.
13. Rüscher, C. H., Phonon spectra of 2:1 mullite in infrared and Raman experiments. *Phys. Chem. Min.*, 1996, **23**, 50–55.
14. Rüscher, C. H., Fritze, H., Borchardt, G., Witke, T. and Schultrich, B., Mullite coatings on SiC and C/C–Si–SiC substrates characterized by infrared spectroscopy. *J. Am. Ceram. Soc.*, 1997, **90**, 3225–3228.
15. Salje, E. and Werneke, Chr., The phase equilibrium between sillimanite and andalusite as determined from lattice vibrations. *Contrib. Mineral. Petrol.*, 1982, **79**, 56–67.
16. Angel, R. J., McMullan, R. K. and Prewitt, C. T., Substructure and superstructure of mullite by neutron diffraction. *Am. Mineral.*, 1991, **76**, 332–342.
17. Voll, D., Lengauer, C., Beran A. and Schneider, H., Infrared band assignment and structural refinement of Al–Si, Al–Ge, and Ge–Ge mullites. *Eur. J. Mineral.*, 2001 (in press).
18. Padlewski, S., Heine, V. and Price, G. D., Atomic ordering around the oxygen vacancies in sillimanite. *Phys. Chem. Min.*, 1992, **18**, 373–378.